Key Engineering Materials Vols. 353-358 (2007) pp. 3100-3103
online at http://www.scientific.net

Online available since 2007/09/10

Intensity of Singular Stress at the End of a Fiber under Pull-Out Force

Nao-Aki NODA[a], Yasushi TAKASE, Ryohji SHIRAO, Jun LI and Jun-Suke SUGIMOTO

Kyushu Institute of Technology, Department of Mechanical Engineering, 1-1 Sensui-cho, Tobata-ku, Kitakyushu, 804-8550 Japan

[a]noda@mech.kyutech.ac.jp

Keywords: Elasticity; Composite Material; Fracture Mechanics; Body Force Method; Singular Integral Equation; Generalized Stress Intensity Factor; Hexagonal Array; Cylindrical Inclusion.

Abstract. In this study, singular stress fields at the ends of fibers are discussed by the use of models of rectangular and cylindrical inclusions in a semi-infinite body under pull-out force . The body force method is used to formulate those problems as a system of singular integral equations where the unknown functions are densities of the body forces distributed in a semi-infinite body having the same elastic constants as those of the matrix and inclusions.Then generalized stress intensity factors at the corner of rectangular and cylindrical inclusions are systematically calculated with varying the elastic ratio, length, and spacing of the location from edge to inner of the body. The effects of elastic modulus ratio and aspect ratio of inclusion upon the stress intensity factors are discussed.

Introduction

In short-fiber-reinforced composites, fibers are mainly used to enhance load carrying capacity by reducing stresses and strains in matrix. However, singular stress appearing at the fiber ends causes crack initiation, crack propagation, and final failure under cyclic loading [1]. To evaluate the mechanical strength of these composites, therefore, it is necessary to know the intensity of those singular stresses. In our previous studies, we have discussed the intensities at the fiber including periodic and zigzag arrays of fibers [2, 3].

Fibers are also used for fracture toughness enhancement. In this aspect, the interaction of a fiber with the matrix in which it is embedded is of great interest. In the previous studies, load transfer from a rod to a surrounding elastic material was originally reported. Experiment on fiber debonding and pullout was studied in detail. Fiber pullout was simulated in terms of a boundary value problem with a finite element method for a circular cylinder with a rigid fiber embedded in its center. Interfacial debonding and frictional sliding associated with the fiber pullout process are two important mechanisms to increase the toughness; and therefore, recent analyses have focused on these mechanisms assuming the bridging law for a cracking in the wake region. However, singular stress appearing at the fiber ends has not been discussed yet in those previous papers although they may cause interfacial initial debonding.

In this paper, fiber pullout is modeled as rectangular and cylindrical inclusions in semi-infinite bodies. Then, the body force method will be used to formulate the problems as a system of singular integral equations. In order to compare the results with the previous solution, tensions of a semi-infinite plate with a fiber and a bonded strip will be also considered. The boundaries will be divided into several intervals, and at each interval unknown body force densities will be approximated accurately by using fundamental densities and power series. Here, the fundamental densities will be chosen to express the singular stress fields exactly [2, 3]. And finally, the intensity of singular stress at the interface edge points will be discussed with varying aspect ratio and elastic modulus ratio of fibers.

Method of analysis

Consider a rectangular inclusion in a semi- infinite plate as shown in Fig.1(a). Here, l_x and l_y are sizes of inclusions, and σ_x^∞ is a stress at infinity. Denote the shear modulus and Poisson's ratio of the matrix by G_M and ν_M and the inclusion by G_I and ν_I. The problem can be expressed as a system of singular integral equations (1) and (2), where the unknowns are body forces densities F_{nM}, F_{tM}, F_{nI}, F_{tI} distributed in the normal and tangential directions along the imaginary boundary in two semi-infinite plates, 'M' and 'I'. Here, the semi-infinite plates 'M' has the same elastic constants as those of the matrix, and the semi-infinite plate 'I' has the same elastic constants as those of the inclusion.

$$-\frac{1}{2}F_{nM}(s_i)-\frac{1}{2}F_{nI}(s_i)+\sum_{k=1}^{2}\Big[\int_{L_k}h_{nn}^{F_{nM}}(r_k,s_i)F_{nM}(r_k)dr_k+\int_{L_k}h_{nn}^{F_{tM}}(r_k,s_i)F_{tM}(r_k)dr_k \quad (i=1,2)$$
$$-\int_{L_k}h_{nn}^{F_{nI}}(r_k,s_i)F_{nI}(r_k)dr_k-\int_{L_k}h_{nn}^{F_{tI}}(r_k,s_i)F_{tI}(r_k)dr_k\Big]=-\sigma_{nM}^{\infty}(s_i)+\sigma_{nI}^{\infty}(s_i)=0 \quad (1)$$

$$\sum_{k=1}^{2}\Big[\int_{L_k}h_{u}^{F_{nM}}(r_k,s_i)F_{nM}(r_k)dr_k+\int_{L_k}h_{u}^{F_{tM}}(r_k,s_i)F_{tM}(r_k)dr_k-\int_{L_k}h_{u}^{F_{nI}}(r_k,s_i)F_{nI}(r_k)dr_k-\int_{L_k}h_{u}^{F_{tI}}(r_k,s_i)F_{tI}(r_k)dr_k\Big]$$
$$=-u_{M,i}^{\infty}+u_{I,i}^{\infty}\quad (i=1,2) \quad (2)$$

Around corner A it is known that the body forces acting on the normal and tangential directions F_n and F_t should be expressed as two types, that is, symmetric mode **I** type $r_1^{\lambda_1-1}$ and skew-symmetric mode **II** type $r_1^{\lambda_2-1}$ to the bisector of the corners. Here, r_1 is a distance measured from the corner **A**, and the eigenvalues λ_1 and λ_2 are given as the roots of eigenequations [4,5]. Table 1 indicates several examples of for corner A, and for corner B. The boundary division is introduced for rectangular inclusion problems because in this problem the fundamental densities are only useful near the corner. The body force densities distributed in the region is expressed as follows using fundamental densities $r_1^{\lambda_1-1}, r_1^{\lambda_2-1}$ and weight functions W_{nM}^{I} - W_{tI}^{II}. Here, the following expressions are shown by taking an example for corner **A** (Equation (3),(4)).

$$F_{nM}(r_1)=F_{nM}^{I}(r_1)+F_{nM}^{II}(r_1)=W_{nM}^{I}(r_1)r_1^{\lambda_1-1}+W_{nM}^{II}(r_1)r_1^{\lambda_2-1},\ F_{tM}(r_1)=F_{tM}^{I}(r_1)+F_{tM}^{II}(r_1)=W_{tM}^{I}(r_1)r_1^{\lambda_1-1}+W_{tM}^{II}(r_1)r_1^{\lambda_2-1}$$
$$F_{nI}(r_1)=F_{nI}^{I}(r_1)+F_{nI}^{II}(r_1)=W_{nI}^{I}(r_1)r_1^{\lambda_1-1}+W_{nI}^{II}(r_1)r_1^{\lambda_2-1},\ F_{tI}(r_1)=F_{tI}^{I}(r_1)+F_{tI}^{II}(r_1)=W_{tI}^{I}(r_1)r_1^{\lambda_1-1}+W_{tI}^{II}(r_1)r_1^{\lambda_2-1} \quad (3)$$

Table 1 Singular index at the corner A and B shown in Fig.1

	corner **A**		corner **B**
	λ_1	λ_2	λ
$G_I / G_M = 2$	0.9109102	0.9788427	0.9630015
$G_I / G_M = 10$	0.7981112	0.7856547	0.8015335
$G_I / G_M = 60$	0.7659920	0.6383511	0.7289061
$G_I / G_M = 100$	0.7632349	0.6218440	0.7219664
$G_I / G_M \to \infty$	0.7590420	0.5951564	0.7111729

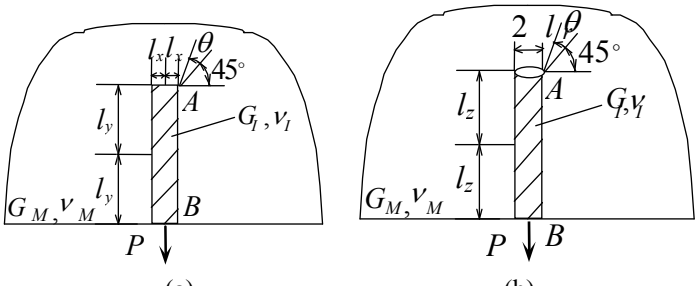

Fig.1 A rectangular inclusion (a) and a cylindrical inclusion (b) in a semi-infinite plate (body) under pullout force

$$W_{nM}^{I}(r_1)=\sum_{n=1}^{M}a_n r_1^{n-1},\ W_{tM}^{I}(r_1)=\sum_{n=1}^{M}b_n r_1^{n-1},\ W_{nM}^{II}(r_1)=\sum_{n=1}^{M}c_n r_1^{n-1},\ W_{tM}^{II}(r_1)=\sum_{n=1}^{M}d_n r_1^{n-1}$$
$$W_{nI}^{I}(r_1)=\sum_{n=1}^{M}e_n r_1^{n-1},\ W_{tI}^{I}(r_1)=\sum_{n=1}^{M}f_n r_1^{n-1}\ W_{nI}^{II}(r_1)=\sum_{n=1}^{M}g_n r_1^{n-1},\ W_{tI}^{II}(r_1)=\sum_{n=1}^{M}h_n r_1^{n-1} \quad (4)$$

Equations (3) and (4) do not include the terms expressing local uniform stretching and shear distortion at the corner **A**. Therefore the stress σ_n^{∞} applied in the plate 'I' is decided to express local uniform stretching and shear distortion at the corner **A**. Except along the boundary, body forces are simply distributed in the normal and tangential directions without using symmetric and skew-symmetric distributions.

On the numerical solution as shown in Equations (3), (4), the singular integral Equations (1), (2) are reduced to algebraic equations for the determination of the unknown coefficients a_n - h_n. These coefficients are determined from the boundary conditions at suitably chosen collocation points. The generalized stress intensity factors K_{I,λ_1}, K_{II,λ_2} for angular corners can be obtained from the values of $W_n^I(0)$, $W_n^{II}(0)$, $W_t^I(0)$, $W_t^{II}(0)$ at the corner tip. In the following discussion, the stress intensity factors $F_{\sigma,I}$, $F_{\sigma,II}$ defined as (5) will be used to express the intensity of singular stress at the corner A. On the other hand, the stress intensity factor F_{σ} defined as (6) will be used to express the one at corner B.

For corner A in Fig.1

$$\sigma_{\theta M}\big|_{\theta=\pm135^\circ}=\sigma_{\theta I}\big|_{\theta=\pm135^\circ}=\frac{K_{I,\lambda_1}}{r^{1-\lambda_1}}f_\theta^I\big|_{\theta=\pm135^\circ}\ \mathrm{m}\ \frac{K_{II,\lambda_2}}{r^{1-\lambda_2}}f_\theta^{II}\big|_{\theta=\pm135^\circ}=\frac{\sigma F_{\sigma,I}}{(r/l_x)^{1-\lambda_1}}\ \mathrm{m}\ \frac{\sigma F_{\sigma,II}}{(r/l_x)^{1-\lambda_2}} \quad (5)$$

For corner B in Fig.1

$$\sigma_{\theta M}\big|_{\theta=90^\circ}=\sigma_{\theta I}\big|_{\theta=90^\circ}=\frac{K}{r^{1-\lambda}}f_\theta=\frac{\sigma F_\sigma}{(r/l_x)^{1-\lambda_2}} \quad (6)$$

Here, we put $\sigma=P/(2l_x)$ (for Fig.1(a)) , $\sigma=P/(\pi l_r^2)$ (for Fig.1(b)) , where P is the magnitute of pullout force.

Numerical results and discussion

Stress intensity factors of a bonded strip and a fiber in a semi-infinite plate under tension. Little results are available for reliable generalized stress intensity factors regarding the edge point B in Fig.1. Therefore, first, we analyzed tension problems for Fig.1 (a), (b) to compare the results each other. Here, a similar method is applied to the bonded strip for Fig.2, whose elastic constants are G_1,ν_1 and G_2,ν_2.

Fig. 2 shows the results for a fiber under transverse tension when l_y/l_x=2, 5, 10. Fig. 2 shows $F_\sigma(B)/F_\sigma(O)$ where $F_\sigma(B)$ is the result at corner B in Fig. 1, and $F_\sigma(O)$ is the result for bonded strip [5]. The value of $F_\sigma(B)/F_\sigma(O)$ decreases with increasingl_y/l_x, and becomes constant as $l_y/l_x\to\infty$. For large value of G_I/G_M, the value becomes smaller. The value of $F_\sigma(B)/F_\sigma(O)$ is mainly controlled by G_I/G_M and insensitive to l_y/l_x.

Stress intensity factors of a fiber under pullout force. For carbon fiber reinforced composites, the elastic modulus ratio is usually in the range of G_I/G_M=61-118, and for glass fiber reinforced composites, G_I/G_M=24-84 [3]. In this analysis, we put G_I/G_M=10 ,60 ,100. Fig. 3 show the results of $F_\sigma(B)$ at the corner B with varying the position

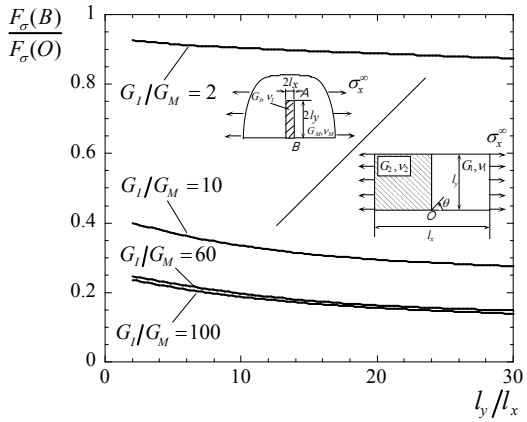

Fig.2 $F_\sigma(B)$ / $F_\sigma(O)$ vs. l_y / l_x

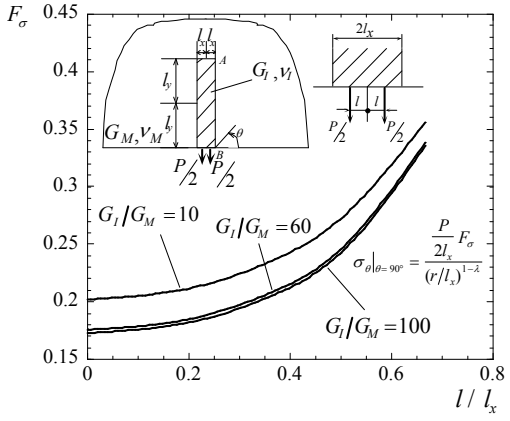

Fig.3 Stress intensity factor $F_\sigma(B)$ for a rectangular inclusion under double pull out forces when l_y / l_x=10

$F_\sigma(B)$: *The result at corner B in semi* – inf *inite plate under tension.*

$F_\sigma(O)$: *The result at corner O in bonded strip plate under tension.*

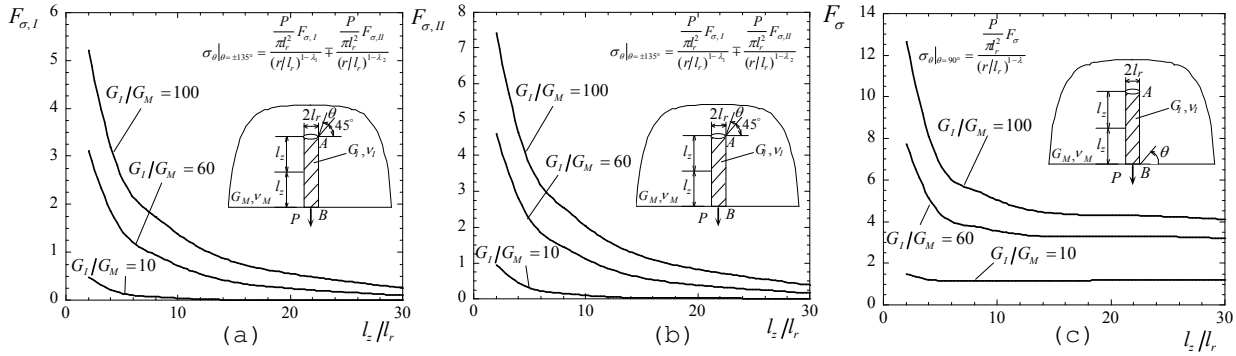

Fig.4 Stress intensity factor (a) $F_{\sigma,I}$(A) ,(b) $F_{\sigma,II}$ (A), and (c) F_σ (B) for a cylindrical inclusion under pull out force

of pullout forces. The value of F_σ increases as the force approaches the corner B. In the range of $0 \le l / l_x \le 2/3$, F_σ becomes larger by 1.9 times. Fig. 4 (a) , (b) , (c) shows the results of cylindrical inclusion under single pullout force. From Fig.4, it is seen that the values of $F_{\sigma,I}$, $F_{\sigma,II}$ approach zero with increasing the aspect ratio l_y / l_x. On the other hand, the value of F_σ for rectangular and cylindrical inclusions becomes constant at $l_y / l_x \cong 10$ for each value of G_I / G_M.

References

[1] H. Nisitani, H. Noguchi and Y.-H. Kim: Engineering Fracture Mechanics Vol.45, No.4 (1993), p.497

[2] N.A. Noda and Y. Takase: ASME Journal of Applied Mechanics Vol.70, No.4 (2003), p.487

[3] N.A. Noda and Y. Takase: International Journal of Solids and Structures Vol.42, No.16-17 (2005), p.4890

[4] D.B. Bogy:Int. J. Solids Structures Vol. 7, No. 8 (1971), p.993

[5] D.H. Chen and H. Nisitani: Transactions of the Japan Society of Mechanical Engineers Series A Vol.59, No.567 (1993-11), p.210